ORIGINAL ARTICLE

Height–diameter allometry for a dominant palm to improve understanding of carbon and forest dynamics in forests of Puerto Rico

Paschalis Chatzopoulos[1,2] | Roel Lammerant[1,3] | Jill Thompson[4] | María Uriarte[5] | Jess K. Zimmerman[6] | Robert Muscarella[1]

[1]Plant Ecology and Evolution, Uppsala University, Uppsala, Sweden

[2]Department of Biology, IVAGRO, University of Cadiz, Cádiz, Spain

[3]Tvärminne Zoological Station, University of Helsinki, Helsinki, Finland

[4]UK Centre for Ecology and Hydrology, Midlothian, UK

[5]Ecology, Evolution, and Environmental Biology, Columbia University, New York, New York, USA

[6]Department of Environmental Science, University of Puerto Rico, Rio Piedras, Puerto Rico, USA

Correspondence
Robert Muscarella, Plant Ecology and Evolution, Uppsala University, Uppsala, Sweden.
Email: robert.muscarella@ebc.uu.se

Abstract

Tropical forests play a major role in the global carbon cycle but their diversity and structural complexity challenge our ability to accurately estimate carbon stocks and dynamics. Palms, in particular, are prominent components of many tropical forests that have unique anatomical, physiological, and allometric differences from dicot trees, which impede accurate estimates of their aboveground biomass (AGB) and population dynamics. We focused on improving height estimates and, ultimately, AGB estimates for a highly abundant palm in Puerto Rico, *Prestoea acuminata*. Based on field measurements of 1003 individuals, we found a strong relationship between stem height and diameter. We also found some evidence that height–diameter allometry of *P. acuminata* is mediated by various sources of environmental heterogeneity including slope and neighborhood crowding. We then examined variability in AGB estimates derived from three models developed to estimate palm AGB. Finally, we applied our novel height:diameter allometric model to hindcast dynamics of *P. acuminata* in the Luquillo Forest Dynamics Plot during a 27-year period (1989–2016) of post-hurricane recovery. Overall, our study provides improved estimates of AGB in wet forests of Puerto Rico and will facilitate novel insights to the dynamics of palms in tropical forests.

Abstract in Spanish is available with online material.

KEYWORDS
aboveground biomass, Arecaceae, environmental heterogeneity, forest dynamics, Neotropics, *Prestoea acuminata* var. *montana* (Graham)

1 | INTRODUCTION

Tropical forests constitute a significant component of the global carbon cycle and are recognized as hotspots of both terrestrial biodiversity and anthropogenic pressure (Malhi et al., 2021; Sullivan et al., 2020). These ecosystems are vital in mitigating climate change due to their capacity to act as carbon sinks by sequestering atmospheric CO_2 as living biomass (Baccini et al., 2012). Accurate quantification of aboveground biomass (AGB) in tropical forests is, therefore, critical to establish baselines and quantify changes in the global carbon cycle (Herold et al., 2019; Ledo et al., 2016).

Emergent technologies in remote sensing are facilitating increasingly rapid and accurate biomass assessments of tropical forests. Nevertheless, the accuracy of these approaches depend on field-based measurements for validation, which presents several challenges (Duncanson et al., 2019; Herold et al., 2019). First, direct measurement of AGB requires destructive harvesting, drying, and weighing of entire (large) plants (Clark & Kellner, 2012). As a result, AGB estimates for trees are typically derived from allometric equations that use nondestructive measurements of stem diameter (D), height (H), and wood density (WD) to predict biomass (Burt et al., 2020; Duncanson et al., 2019; Zuleta et al., 2022). Second, accurate measurement of height—a critical input of many AGB models—is challenging and time consuming, especially in dense tropical forests (Larjavaara & Muller-Landau, 2013). As a result, allometric sub-models that predict height from measured diameter are often components of models that estimate AGB (Burt et al., 2020; Chave et al., 2004; Ledo et al., 2016; Molto et al., 2013).

Although strong height:diameter (H:D) relationships exist for many trees due to coupled primary and secondary growth (Niklas, 2004), these relationships can vary across species and environmental conditions (Chave et al., 2014; Feldpausch et al., 2011, e.g., Avalos et al., 2019). However, arborescent palms, which are highly abundant members of many Neotropical forests (Dalagnol et al., 2022; Hastie et al., 2022; Muscarella et al., 2020; ter Steege et al., 2013), do not necessarily exhibit strong H:D relationships. More precisely, palms—as monocots—do not undergo "true" secondary growth; instead, they increase in diameter through a process described as "sustained primary growth," which involves the enlargement of parenchyma cells throughout the stem with lignification and increased thickness of cell walls (Tomlinson, 1990). As a result, palms achieve tall heights without producing secondary xylem by "overbuilding" their stems at early ontogeny in order to facilitate future growth (Avalos et al., 2019, 2022; Niklas, 1992; Tomlinson, 1990). Some palms also produce fibers with thick cell walls as a mechanism for attaining considerable heights without secondary growth. For some palm species, therefore, these growth mechanisms can decouple height and diameter associations, which can reduce accuracy of AGB estimates in tropical forests where palms account for a substantial proportion of stems (Goodman et al., 2013; Muscarella et al., 2020).

Even in cases where strong H:D relationships can be established, variation in environmental conditions can affect allometric scaling through patterns of resource availability or effects on the local competitive environment (Avalos et al., 2019; Feldpausch et al., 2011; Weiner, 2004). For example, trees growing on steeper and drier slopes had shorter stems for a given diameter in a wet evergreen monsoon forest in India (Antin et al., 2013). Trees in French Guiana's rainforest were more slender on hilltops than in bottomlands, likely as a result of variation in local stand density and competition for light (Ferry et al., 2010). For palms, Avalos et al. (2019) showed variation of H:D allometry for palms from different forest strata and geographic locations, but the underlying causes for this variation are unclear. A better understanding of H:D relationships for palms, including potential influences of environmental heterogeneity, would improve estimates of tropical forest biomass and enhance understanding of the factors that mediate palm growth, population dynamics, and responses to disturbance.

We developed a novel H:D allometric equation for an abundant palm on the island of Puerto Rico, *Prestoea acuminata* (R. Graham) Nichols. Our core motivation is that the existing AGB model for this species (Frangi & Lugo, 1985) requires stem height as an input, which is rarely measured. We apply our novel H:D allometric model in conjunction with existing AGB models to hindcast AGB dynamics in the Luquillo Forest Dynamics Plot over a 27-year period (1989–2016), spanning a period of hurricane recovery. We address the following questions:

1. Does *P. acuminata* exhibit a height–diameter (H:D) relationship and, if so, what is the best model to fit this relationship?

While the lack of true secondary growth in palms can decouple diameter and height, sustained primary growth can lead to significant H:D relationships for some species (Avalos et al., 2019; Goodman et al., 2013). Based on field measurements of diameter and height, we compared a suite of models to predict stem height from stem diameter for *P. acuminata*.

2. How does environmental heterogeneity mediate H:D allometry of *P. acuminata*?

We quantified the slenderness ratio of each palm (H/D) to test how allometry of *P. acuminata* varies with elevation, slope, and neighborhood crowding (reflecting the competitive light environment). We predicted that palms would be less slender at higher elevations due to wetter conditions and more exposure to wind. We also expected palms on steeper slopes to be less slender if slope serves as a proxy for water availability; steeper slopes are associated with drier soils which could select for more stout palms. Finally, we predicted that palms growing in more crowded areas would be more slender due to greater competition for light.

3. How variable are palm aboveground biomass (AGB) estimates based on available models?

We evaluated the variability of estimated AGB for *P. acuminata* using three models of palm AGB: a species- and site-specific model (Frangi & Lugo, 1985) coupled with our newly developed H:D model, and two family-level models for palms developed by Goodman et al. (2013) and Avalos et al. (2022).

4. How has AGB of *P. acuminata* changed during a 27-year period following a major hurricane?

To further understand palm and forest dynamics after major hurricane disturbance, we used our novel H:D model to hindcast palm AGB for the Luquillo Forest Dynamics Plot over a 27-year period (1989–2016), following the Category 4 hurricane Hugo in 1989. Because hurricanes tend to impose higher levels of damage on non-palm trees compared to palms (Uriarte et al., 2019, Zhang et al., 2022a, 2022b, Uriarte et al., 2023), we expected an increase in palm relative abundance and AGB over this period.

2 | METHODS

2.1 | Study site and focal species

We used new and existing data from the 16-ha Luquillo Forest Dynamics Plot (LFDP) and its immediate surroundings, situated in northeastern Puerto Rico. The LFDP ranges in elevation from 337 to 425 m, has a slope ranging from 3% to 65%, and receives an average annual precipitation of ca. 3500 mm yr^{-1} (Thompson et al., 2002). The LFDP has been exposed to various natural and anthropogenic disturbances which, in combination with variation in soil types and terrain, has generated a highly heterogeneous physical environment (Thompson et al., 2002; Zimmerman et al., 2021). Approximately every 5 years since 1990, all free-standing woody plants in the LFDP with a diameter at breast height (DBH) ≥1 cm are measured, identified, mapped, and tagged (notably, measurements of plant height are not included in the LFDP census protocol).

Prestoea acuminata (var. *montana*; Sierra palm) is a medium-size arborescent palm widespread and abundant in wet forests of Puerto Rico and, by far, the most abundant and widespread palm species in Puerto Rico, including in the LFDP (Miller & Lugo, 2009). Many forests of Puerto Rico are dominated by *P. acuminata*; in 2016, for example, *P. acuminata* accounted for 22% of the total stems and 23% of the total basal area in the LFDP. *P. acuminata* can be found on steep slopes and alongside streams and waterlogged soil on mountain floodplains (Frangi & Lugo, 1998, Lugo & Frangi, 2016).

We used data from the six LFDP censuses available at the time of our study (i.e., those completed in 1990, 1994, 2000, 2005, 2011, and 2016), accessed with the EDIutils R package (Smith, 2022). This time series spans a period immediately following a major hurricane (Hugo 1989) and including several less severe hurricanes (e.g., Georges in 1998, Irene in 2011) but preceding a major hurricane (Maria) that decimated the island in 2017. Additionally, we measured the diameter and height of a subset of palms inside the LFDP (*n* = 882), as well as a haphazard sample of 121 palms in the area immediately adjacent to the LFDP, in January 2020 (total *N* = 1003 palms). For each palm, we measured stem height from the ground to the base of the crown (H_{bc}; height of the youngest internode), diameter at 130 cm aboveground (D_{130}), and basal diameter (D_B; just above the top of the roots) (Figure S1). For palms with H_{bc} ≤2 m, we measured height with a measuring tape, for palms between 2 and 5 m tall, we used a calibrated extension pole, and for palms >5 m, we used a Nikon forestry Pro II rangefinder.

2.2 | Height–diameter allometry

To address Q1, we compared a suite of allometric equations (Table 1) to find the best fit model that predicts *P. acuminata* H_{bc} as a function of D_{130}, following previous studies (e.g., Ledo et al., 2016). We fit models 1–3 and 5–6 using the *lm* function and Model 4 using the *nls* function in R v4.1.3 (R Development Core Team, 2020), and Model 7 using the BIOMASS R package (Réjou-Méchain et al., 2017). We used cross-validation to assess model performance by splitting the data into training and validation sets of 63% and 37%, respectively (Xu & Goodacre, 2018). Across 100 bootstrap iterations, we calculated the median and standard deviation of root mean square error (RMSE), residual standard error (RSE), and R^2. We also calculated the Akaike Information Criterion (AIC) with the full dataset and considered the model(s) with ΔAIC <2 as the best model(s) (Johnson & Omland, 2004). We adjusted AIC values for models with a log-transformed response variable as: $AIC_{adj} = AIC + -2 \sum \log\{y(n) + 1\}$ (Akaike, 1978). We do not provide R^2 for the power law or Weibull models, because this metric is inappropriate for non-linear models (KvaLseth, 1983). Models with lower AIC, RMSE, RSE and higher R^2 performed better; we selected the 'best' model based on lowest AIC and consideration of other evaluation statistics. We used the same approach to compare models of D_B and H_{bc}. For all models that predicted $\log(H_{bc})$, we used the "logbtcf" function from the FSA R package (Ogle et al., 2023) to compute a correction factor as defined by Sprugel (1983) to correct for bias introduced by log-transformation.

2.3 | Environmental heterogeneity and its effects on palm allometry

To investigate the influence of environmental heterogeneity on palm allometry (Q2), we first computed the slenderness ratio ($H_{bc}:D_{130}$ ratio) for each palm. For palms inside the LFDP, we used the LFDP census data to determine elevation (m) and slope (%) in their immediate area (Thompson et al., 2002; Zimmerman, 2018). We excluded palms outside the LFDP from this analysis. To assess how local biotic

TABLE 1 The suite of allometric models used to mathematically describe height at the base of the crown (H_{bc}; m) as a function of diameter (D_{130} or D_B; cm).

Model	Functional form
1. Linear	$H_{bc} = a + b \times D$
2. Log-linear	$H_{bc} = a + b \times \ln(D)$
3. Log–log	$\ln(H_{bc}) = a + b \times \ln(D)$
4. Power law	$H_{bc} = a + D^b$
5. Log–log quadratic I (single term)	$\ln(H_{bc}) = a + b \times \ln(D)^2$
6. Log–log quadratic II (two term)	$\ln(H_{bc}) = a + b \times \ln(D) + c \times \ln(D)^2$
7. Weibull	$H_{bc} = a \times \left(1 - \exp\left(-\left(\frac{D}{b}\right)^c\right)\right)$

Note: The parameters *a*, *b*, and *c* are model coefficients.

conditions influence palm allometry, we computed a neighborhood crowding index (NCI) based on the density and size of trees in a 20 m radius surrounding each focal palm, following Uriarte et al. (2004). Specifically, we computed NCI as the sum of the ratio of DBH of each j neighboring tree divided by its distance from the i focal tree:

$$NCI_i = \sum_{i=1, \ i \neq j}^{j} \frac{DBH_j}{dist_{ij}} \qquad (1)$$

To minimize edge effects, we excluded palms located <20 m from the LFDP boundary, leaving 726 palms for this analysis. We then used multivariate regression to relate slenderness ratio with elevation (m), slope (%), and log-transformed NCI.

2.4 | Biomass model comparison and AGB hindcasting

We used three palm-specific models to assess the magnitude of variation of their AGB estimates (Q3). We first used these models for individual AGB estimates of our 1003 sampled palms and then for palm AGB in the LFDP during each census. As a baseline for comparison, we used the species- and site-specific AGB model developed by Frangi and Lugo (1985), which was parameterized by regressing measured AGB and height of harvested *P. acuminata* individuals from a nearby site with similar conditions as the LFDP. This model takes the form:

$$\widehat{AGB} = 4.5 + 7.7 \times H_{bc} \qquad (2)$$

For our 1003 sampled palms, we used our measured height data (H_{bc}) with this model. When applying this model to the LFDP census data, we first estimated H_{bc} based on field measured D_{130} and our best fit $H_{bc}:D_{130}$ model. We estimated upper and lower bounds for total palm AGB in each census based on the 95% confidence intervals of H_{bc} predicted by our $H_{bc}:D_{130}$ model.

We compared estimates of palm AGB based on Equation 2 with estimates from a 'family-wise' AGB model of Goodman et al. (2013), developed with data from eight Amazonian palm species (not including *P. acuminata*). The Goodman et al. (2013) model takes the form:

$$\ln\left(\widehat{AGB}\right) = -3.3488 + 2.7483 \times \ln(D_{130}) \qquad (3)$$

We selected this particular model for comparison because it is based on measured D_{130} and does not require information on height. Note, however, that Goodman et al. (2013) also provide a family-wise model that includes terms for stem height and dry mass fraction which provided a better fit to their data.

Finally, we also compared palm AGB estimates from a "family-wise" model of aboveground carbon from Avalos et al. (2022). This model was parameterized for eight Costa Rican palm species and takes the form:

$$\ln\left(\widehat{AGC}\right) = -4.77 + 2.82 \times \ln(D_{130}) \qquad (4)$$

Note that Equation 4 predicts aboveground carbon (not biomass) so we used a conversion factor of 2 to convert to dry biomass, following Avalos et al. (2022). Additionally, predictions of AGB were multiplied by a correction factor of 1.4 to compensate for introduced bias due to log-transformation (see Avalos et al., 2022).

To address Q4, we used estimates for total palm AGB in the LFDP as described above but we only included palms that had a diameter measured at between 1 and 1.6 m above the ground as our H:D model was fit with D_{130} values. To express palm AGB as a fraction of total tree AGB in the LFDP, we used the BIOMASS R package (Réjou-Méchain et al., 2017) to estimate AGB for all non-palm trees.

3 | RESULTS

3.1 | H:D allometry

The palms we measured ranged in D_{130} from 6.4 to 21.9 cm, which corresponds well to the overall range of variation for palm DBH in the LFDP (Figure S2). The best fit model (i.e., lowest AIC) was the log–log quadratic with a single term (Table 2, Model 5):

$$\widehat{H_{bc}} = 1.068344 * \exp\left(-1.26 + 0.40 \times \ln(D_{130})^2\right) \qquad (5)$$

Other evaluation statistics of this model were better or comparable to the other models (Table 2). All linear models were significant ($p < .001$) based on F-tests. Although F-tests are not valid for non-linear models, all coefficients in these models were statistically significant and their confidence intervals did not overlap zero. Model comparison metrics show that log-transformation of both H_{bc} and D_{130} resulted in better fit models, consistent with previous studies that rejected linear, log-linear, and parametric models (Feldpausch et al., 2011). Unsurprisingly, linear and log-linear models tended to underestimate height and predict negative height estimates for small individuals, whereas the simple log-model underestimated height for taller palms (Figure 1a).

A detailed summary of fitted $H_{bc}:D_B$ models is presented in Table 2. The log–log quadratic model II (two-term; Model 6b in Table 2) provided the best fit (Figure 1b):

$$\widehat{H_{bc}} = 1.065064 * \exp\left(6.207 - 4.937 \times \ln(D_B) + 1.052 \times \ln(D_B)^2\right) \qquad (6)$$

This model explained slightly more variation ($R^2 = 0.57$ vs. 0.55) and, more importantly, could be used to fit shorter palms than models based on D_{130}.

3.2 | Allometry and environmental heterogeneity

Our analysis of the slenderness ratio ($H_{bc}:D_{130}$) of *P. acuminata* revealed weak but statistically significant associations with slope and

TABLE 2 Model comparison and goodness-of-fit statistics, and parameter estimates, for the suite of allometric models of $H_{bc}:D_{130}$ (top rows) and $H_{bc}:D_B$ (bottom rows) for *P. acuminata* in the Luquillo Forest Dynamics Plot, Puerto Rico ($N = 1003$).

Diameter	Model	AIC	ΔAIC	R²	RSE	RMSE (sd)	a	b	c	Correction factor
D_{130}	(1) Linear	4067.6	342.1	0.52	1.83	1.83 (0.07)	−5.46 (0.00)	0.78 (0.00)	–	NA
	(2) Log-linear	4120.2	394.7	0.50	1.88	1.88 (0.07)	−20.04 (0.00)	9.72 (0.00)	–	NA
	(3) Log-log	3732.9	7.4	0.55	0.36	4.18 (0.12)	−3.90 (0.00)	2.08 (0.00)	–	1.068867
	(4) Power law	4062.3	336.8	–	1.83	1.83 (0.08)	0.02 (0.00)	2.12 (0.00)	–	NA
	(5) Log-log quadratic I (single term)	3725.5	0.0	0.55	0.36	4.18 (0.11)	−1.30 (0.00)	0.42 (0.00)	–	1.068344
	(6) Log-log quadratic II (two terms)	3726.5	1.0	0.55	0.36	4.18 (0.11)	0.05 (0.97)	−1.08 (0.32)	0.63 (0.00)	1.068346
	(7) Weibull	4756.3	1030.7	–	69.41	1.92 (0.07)	12.73 (0.00)	15.9 (0.00)	3.38 (0.00)	NA
D_B	(1b) Linear	4058.4	384.3	0.52	1.85	1.86 (0.11)	−4.57 (0.00)	0.34 (0.00)	–	NA
	(2b) Log-linear	4122.2	448.1	0.48	1.91	1.92 (0.10)	−24.49 (0.00)	8.87 (0.00)	–	NA
	(3b) Log-log	3707.3	33.2	0.56	0.36	4.14 (0.13)	−4.99 (0.00)	1.94 (0.00)	–	1.067408
	(4b) Power law	4040.4	366.3	NA	1.83	1.84 (0.11)	0.01 (0.00)	1.97 (0.00)	–	NA
	(5b) Log-log quadratic I (single term)	3690.4	16.2	0.56	0.36	4.14 (0.13)	−1.85 (0.00)	0.30 (0.00)	–	1.066235
	(6b) Log-log quadratic II (two terms)	3674.1	0	0.57	0.36	4.13 (0.13)	6.207	−4.94 (0.00)	1.05 (0.00)	1.065064
	(7b) Weibull	4835.6	1161.5	NA	154.98	1.96 (0.07)	14.11 (0.00)	37.48 (0.00)	2.44 (0.00)	NA

Note: Standard deviation is provided for model RMSE as the mean of 100 bootstrap iterations. Estimated coefficients (*a*, *b*, *c*) correspond to the functional forms shown in Table 1; *p*-values are given for each coefficient. Correction factors for models with log-transformed response variables follow Sprugel (1983). All linear models were significant ($p < .001$) based on *F*-tests. *F*-tests are not valid for nonlinear models (4 and 7) but all coefficients were statistically significant and confidence intervals did not overlap zero.
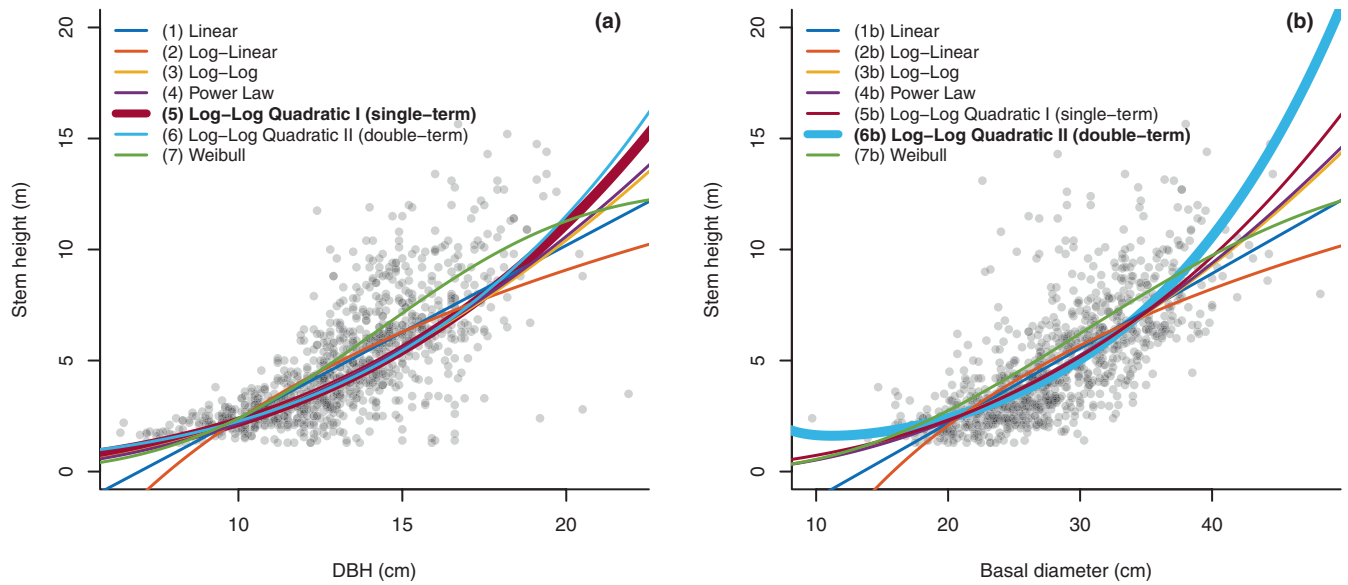
FIGURE 1 Fitted (a) H_{bc}:D_{130} and (b) H_{bc}:D_B allometric models for *P. acuminata*. Each point represents an individual palm and each line a fitted allometric model. The applicable range is 1.30 m ≤ H_{bc} ≤ 14.75 m and (a) 6.4 cm ≤ D_{130} ≤ 21.9 cm, (b) is 9.7 cm ≤ D_B ≤ 48.2 cm. The best fitted model in (a) is the Log–log quadratic I (single term; Model 5 from Table 2) and in (b) is the Log–log quadratic II (two-term; Model 6 from Table 3).

TABLE 3 Goodness-of-fit statistics and estimated coefficients (with *p*-values) for multiple linear regression between slenderness ratio (H_{bc}:D_{130}) and environmental conditions for *P. acuminata* (N = 726) in the Luquillo Forest Dynamics Plot, Puerto Rico.

Model	R^2	RSE	Intercept	Elevation	Slope	NCI
SR ~ Elevation + Slope + $\log_{10}$(NCI)	0.03	14.0	37.3 (<0.001)	0.66 (0.22)	−1.07 (0.04)	−1.85 (<0.001)

Note: Coefficients are based on a model fitted with covariates centered on their mean and scaled to unit standard deviation (overall model statistics: F = 6.48, *p*-value <.001).

neighborhood crowding (NCI), but not elevation (Table 3; F = 6.48, *p* < .001). Specifically, palms in steeper terrain and in more crowded conditions (greater NCI) tended to be less slender (Figure 2). Although these effects were statistically significant, the model explains little of the total variation in the dataset (R^2 = 0.03), indicating overall weak associations between palm allometry and the gradients in our dataset (Table 3).

## 3.3 | Influence of model selection on biomass estimates

Compared to the baseline model of Frangi and Lugo (1985), the Goodman et al. (2013) model tended to overestimate AGB of individual palms by an average of 2.42 kg (±16.41 sd) while the Avalos et al. (2022) model tended to underestimate AGB of individual palms by an average of 5.00 kg (±14.95 sd) (Figure 3). Summed across all palms in our dataset, the value of total palm AGB estimated with the Goodman et al. (2013) model was 9.3% higher than the baseline estimate whereas the estimate from the Avalos et al. (2022) model was 10.6% lower than the baseline.

For estimated palm AGB in the LFDP, the range between the upper and lower bounds (based on 95% confidence intervals of

height from our H:D model) corresponded to ~6% of the total estimated palm AGB based on the baseline Frangi and Lugo (1985) model (see error bars in Figure 4). Estimates of palm AGB from the Goodman et al. (2013) model were 17%–23% higher than the baseline, depending on the census. In contrast, the Avalos et al. (2022) model estimates were similar to the baseline, with values varying ca. 3% from the baseline and lying within the upper and lower bounds of the baseline model.

3.4 | Biomass dynamics

Relative abundance of *P. acuminata* followed a steadily increasing trend in the LFDP during the period covered by our study, rising from 4.6% of total stems in 1990 to 22.0% in 2016 (Figure 5). Until the 2000 census, *P. acuminata* was the fifth most prevalent species while in the census of 2005 it ranked second and during the last two censuses (2011 and 2016), it was the most abundant species in the LFDP. Accordingly, the relative basal area of *P. acuminata* increased from 13.4% in 1990 to 22.5% in 2016. These patterns were mirrored by an upward trend in *P. acuminata* AGB estimates (Mg/ha) throughout the censuses. Total estimated palm AGB in the LFDP increased by 81% over the study period, from 15.0 Mg/ha in 1990 to 27.2 Mg/
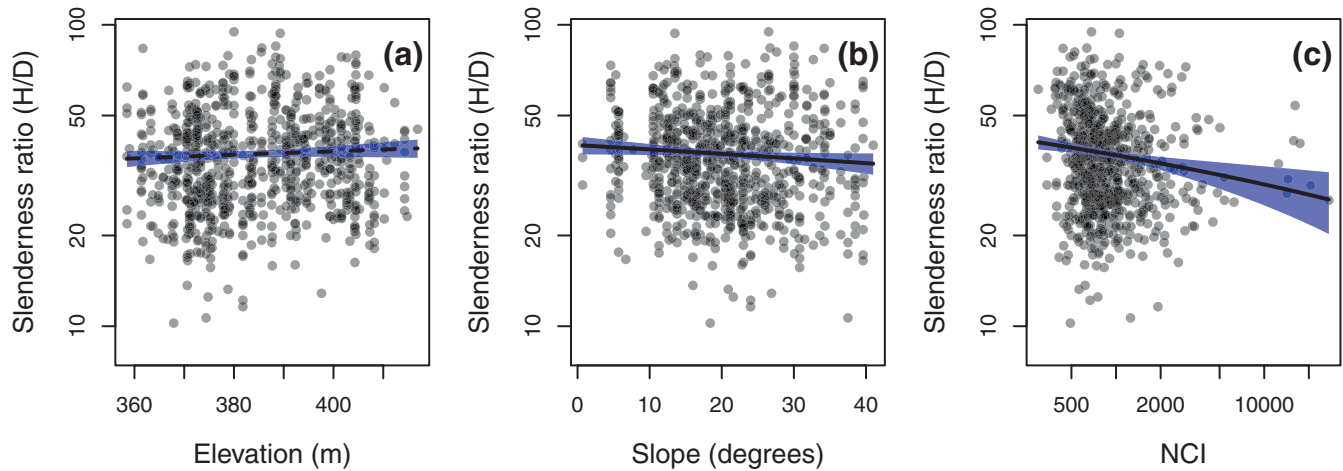
FIGURE 2 Variation of palm slenderness ratio (height/diameter) across gradients of (a) elevation, (b) slope, and (c) the neighborhood crowding index (NCI). Each point represents an individual palm; lines show predicted relationships based on multiple OLS regression, shaded areas show 95% confidence intervals. Solid (dashed) lines represent statistically significant (nonsignificant) slopes. Details of regression fits are provided in Table 3.

ha in 2016 (Figure 4). In 1989, we estimated that *P. acuminata* accounted for ~5% of total AGB in the LFDP; a value that nearly doubled by 2016 (Figure 5).

4 | DISCUSSION

We aimed to improve height estimates—as a major component for predicting biomass and forest dynamics—for a highly abundant palm in Puerto Rico. Specifically, we established a new site- and species-specific model to predict stem height from diameter for *P. acuminata*, which can be used to more accurately estimate biomass dynamics. The effects of environmental heterogeneity on allometry were weak in our dataset but we found some evidence that palm slenderness is influenced by slope and neighborhood crowding. Besides helping to improve biomass estimates, this finding may also shed light on factors influencing palm growth. Overall, our study demonstrates the utility of developing allometric relationships for individual palm species to improve understanding of forest dynamics, especially in areas like Puerto Rico, where palms are highly abundant.

4.1 | H:D allometric models

The log–log quadratic version of the ordinary least square (OLS) model with a single term provided the best fit for the H_{bc}:D_{130} whereas the log–log quadratic with two terms proved best fit for the H_{bc}:D_B relationship. Significant *H:D* relationships are convenient for facilitating biomass estimates but may also shed light on growth mechanisms for this species. Notably, the H_{bc}:D_{130} scaling exponent, slope of logarithmic OLS model (Table 2, Model 3) found for *P. acuminata* ($b = 2.018$) is very similar to that of a congeneric species in Costa Rica, *Prestoea decurrens* ($b = 2.18$) (Avalos et al., 2019). These concordant results suggest the potential for phylogenetic

conservatism in H:D scaling relationships, which could support the use of more general models (e.g., genus-level) when species-specific models are not available (e.g., the model of aboveground carbon developed for *P. decurrens* by Avalos et al. (2022)). Overall, future work evaluating the phylogenetic signal of allometric relationships may prove useful for developing and selecting models used in biomass estimations, and for understanding variation in palm growth mechanisms across species.

Although less commonly measured in field inventories, basal diameter (D_B) provided a slightly better prediction of stem height ($R^2 = 0.57$ compared to 0.55 for D_{130}) in our dataset (Equation 6). Many field protocols either exclude standing palms <1.3m tall in part because D_{130} cannot be measured or they measure diameter at different heights (including the current LFDP protocol). For example, in our dataset, H_{bc}: D_{130} models are trained with palms of height greater than 1.3m while H_{bc}:D_B with palms $0.4 \leq H_{bc}$. However, basal diameter can be relatively easily measured and used to predict height (and, ultimately, biomass) of shorter palms, thereby offering a more comprehensive census and stand-level estimate of biomass than possible with D_{130}. Overall, we advocate that field inventories in sites where palms are abundant (e.g., the LFDP) consider incorporating methodological accommodations to account for the morphological diversity of palms (e.g., consider measuring palm basal diameter, perhaps in addition to D_{130}).

4.2 | Environmental heterogeneity and palm allometry

We evaluated how environmental conditions mediate palm allometry by assessing relationships between elevation, terrain slope, and neighborhood crowding (NCI) on the slenderness ratio of palms in the LFDP. Previous work has shown that abundance of *P. acuminata* can depend on edaphic conditions such as soil properties and
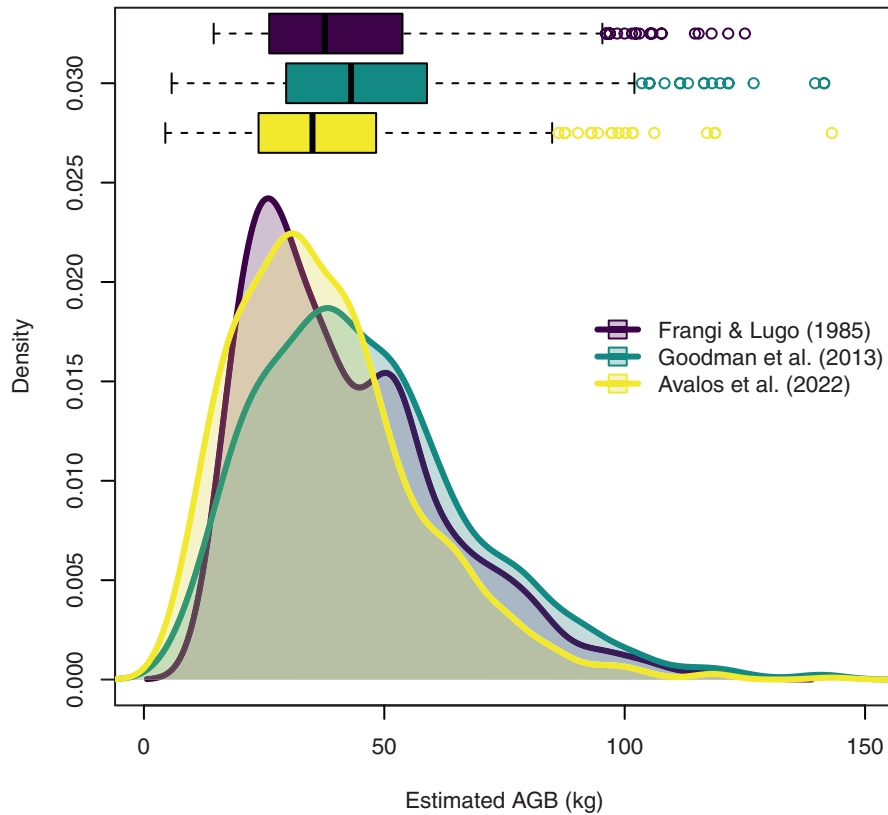
FIGURE 3 Comparison of estimated AGB based on different models for sampled individuals of *P. acuminata* in the Luquillo Experimental Forest, Puerto Rico. Density plots show distribution of estimated AGB across all 1003 individual palms measured in our study based on the 'baseline' model of Frangi and Lugo (1985) using measured stem height, the family-wise model of Goodman et al. (2013) (based on stem diameter only), and the family-wise model of Avalos et al. (2022) (based on stem diameter only). Boxplots summarize the distributions; boxes show the 25th percentiles, medians, and 75th percentiles; horizontal bars show the interquartile range × 1.5; datapoints beyond these bars are outliers.
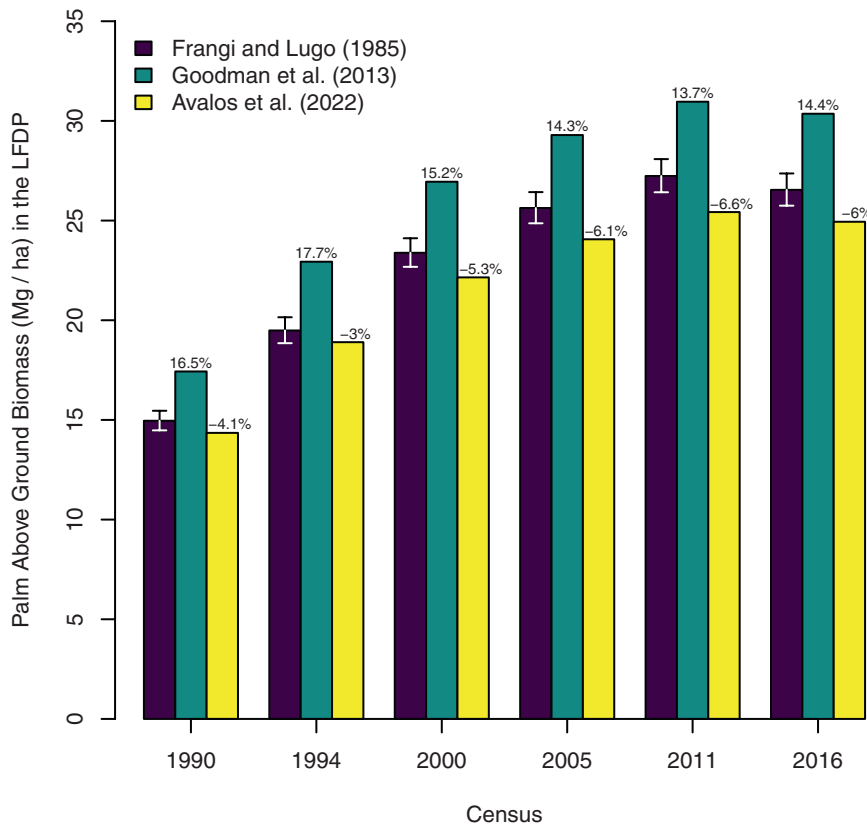

FIGURE 4 Comparison of estimated AGB of *P. acuminata* using three alternative models for the Luquillo Forest Dynamics Plot, Puerto Rico. Purple (leftmost) bars reflect estimates based on the site- and species-specific model for *P. acuminata* AGB from Frangi and Lugo (1985) and the $H:D_{130}$ model developed in this study. Error bars reflect the upper and lower bounds based on the upper and lower 95% confidence intervals of our $H:D_{130}$ model. Green (center) bars reflect estimates based on the family-wise model from Goodman et al. (2013), considering D_{130} only. Yellow (rightmost) bars reflect estimates based on the family-wise model from Avalos et al. (2022), again considering D_{130} only. Values shown on top of bars indicate the % difference of estimates compared to the baseline Frangi and Lugo (1985) model.

groundwater access, with higher abundance observed in higher elevation mountain floodplain forests and soil with higher concentration of Ca and Mg (Frangi & Lugo, 1998; Johnston, 1992). The effects of such factors on allometry have, however, not been addressed.

Although the effect was weak, palms growing in relatively flat areas tended to reach somewhat taller heights for a given diameter (i.e., more slender) compared to palms growing on steep slopes. We interpret these differences in the context of water availability.
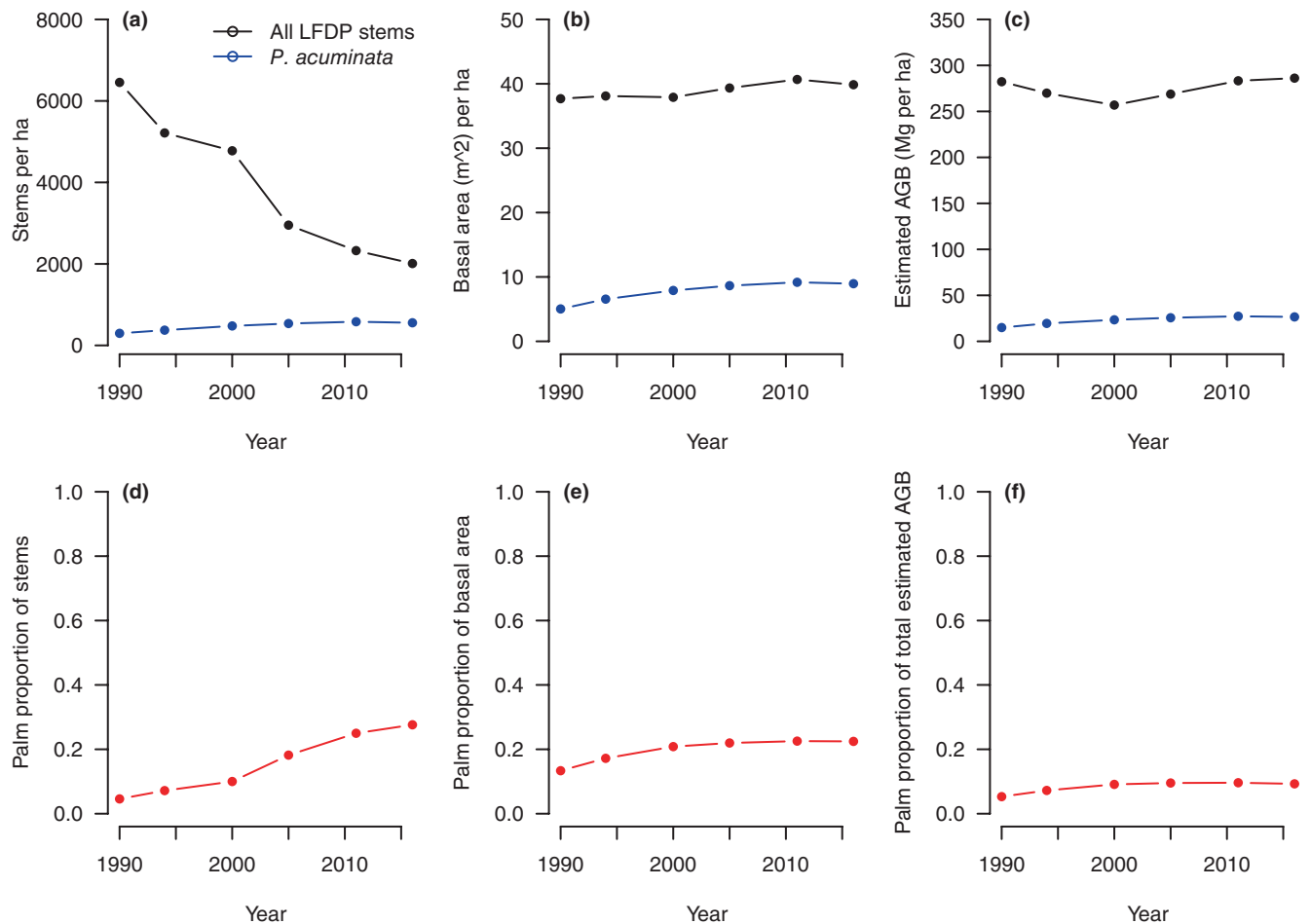
FIGURE 5 Changes in (a, d) stem density, (b, e) basal area, and (c, f) estimated aboveground biomass (AGB) for all stems in the Luquillo Forest Dynamics plot during 1989–2016. Upper panels show absolute changes in total values (all stems) and values for *P. acuminata* only. Lower panels show changes in the proportion of *P. acuminata* for these metrics.

Specifically, steep slopes tend to have thin and rocky soils with lower water-holding capacity compared with flat areas, which tend to have deeper soils with larger water reserves (e.g., Antin et al., 2013). Lower water (and potentially nutrient) availability on steep slopes may select for relatively short and stout palms. It is also possible that greater exposure to hurricanes on steep slopes may select for stouter palms compared to flatter areas, which are often more protected from hurricanes (unless the flat area is on a ridge).

We also observed that palms growing in less crowded neighborhoods (lower NCI) tended to be slightly taller for a given stem diameter. As with slope, the association was weak but we interpret this result as a potential signal of rapid vertical growth following gap openings and consequent increased light availability. As discussed above, palms first increase in diameter and later in height, which leads to an understory rich in short palms, which then grow rapidly in height when a disturbance (e.g., canopy gaps or hurricanes) allows light to penetrate the understory. *P. acuminata* is a mid-successional species and its growth is highly regulated by light availability thus can make the most out of an open environment such that it can increase stem height rapidly when light is available (Weaver, 2010).

In contrast, we did not find a statistically significant effect of elevation on palm allometry. We note, however, that the range of

elevation covered in our study was limited (359–417 m) compared to the elevational range of *P. acuminata* in Puerto Rico, which spans from 60 to 1000 m above sea level (Miller & Lugo, 2009). Any potential effect of elevation on palm allometry may thus be more apparent across a broader range of elevation, which would capture greater differences in exposure to wind disturbance and precipitation. Overall, although the effect of environmental heterogeneity on palm allometry was weak, our study is consistent with some previous work (e.g., Duncanson et al., 2015) suggesting value in considering environmental effects when developing allometric models for species that span broad gradients. Future work may benefit from investigating allometric variation across broader environmental gradients or using longitudinal studies, which could be more appropriate for measuring the development of slenderness ratio over time.

4.3 | Palm AGB model comparison

To date, quantifying palm AGB stocks and dynamics for the LFDP has been challenged by the requirement of height as an input to the existing site- and species-specific AGB model of Frangi and Lugo (1985). We therefore focused on parameterizing a model to

estimate height from stem diameter. Compared to our local "baseline" (i.e., the Frangi and Lugo (1985) model with measured height values), the palm family model of Goodman et al. (2013) tended to overestimate AGB. Critically, the Goodman et al. (2013) model was fitted with Amazonian palm species (some of which did not display a linear H:D relationship), not including *P. acuminata*, and under different climatic and environmental conditions. On the other hand, Frangi and Lugo's (1985) model was built specifically for *P. acuminata* and was parameterized with palms harvested from the Luquillo mountains. The Avalos et al. (2022) family-wise model (also based on a set of seven Neotropical palm species, not including *P. acuminata* but including a congeneric species, *P. decurrens*) tended to underestimate AGB for our measured palms compared to the baseline. However, this model provided similar estimates as the baseline model for the LFDP census data. The discrepancy between models for our different datasets (i.e., our field measured palms and the LFDP census data) is likely due, in part, to the different size distributions palms in the field data versus the LFDP census data (i.e., a higher relative proportion of large D_{130} palms in the LFDP census data compared to our field measured dataset). The discrepancy of AGB estimates among candidate models overall may emerge from (1) different size distributions of palms used to parameterize each model (e.g., the Goodman et al. (2013) model is parameterized for $H > 3\,m$ and $6 \leq D_{130} \leq 40\,cm$; this information is not provided for the Frangi and Lugo (1985) model), and (2) each model is parameterized for different species, in different locations, and thus also encapsulates different environmental gradients. For future work on this species in Puerto Rico, we recommend using the Frangi and Lugo (1985) model in conjunction with either measured height or height estimated from our best fit model (Equation 5). Overall, we encourage the use of models parameterized with individuals from the same region that best represent local environmental variation.

4.4 | Palm dynamics

By integrating our new $H_{bc}{:}D_{130}$ model, we provide novel estimates of palm AGB dynamics in the LFDP during the 1989–2016 study period. In particular, after the passage of hurricane Hugo in 1989, palm AGB, relative abundance and relative basal area reached a plateau 22 years after and then exhibited a small decrease. Since the 2016 census, three catastrophic hurricanes, Irma and Maria in 2017, and Fiona in 2022, have impacted the LFDP but the extent of these effects are not captured by our data. Uriarte et al. (2019), however, specifically examined the impact of Hurricane Maria and indicated that the steam breakage for *P. acuminata* was only 5%, a far lower rate compared to non-palm trees, which experienced a 29% breakage. Moreover, Uriarte et al. (2023) showed that, at the landscape scale, *P. acuminata* density was positively associated with past hurricane exposure. These findings suggest high resistance and resilience of palms to hurricanes (Canham et al., 2010; Frangi & Lugo, 1991). Our results are consistent with future scenarios that predict an increase of palm AGB due to hurricane intensification and

low hurricane-induced palm mortality (Zhang et al., 2022a, 2022b). Continued monitoring will provide insights to the long-term trajectory of palms in this forest, especially under a changing environment with intensified hurricane events.

5 | CONCLUSIONS

Improving the accuracy of biomass estimates in tropical forests is critical for understanding the global carbon balance. Our study highlights the importance of developing palm-specific allometric models for tropical forest sites, such as the Luquillo Forest, where palms are abundant and constitute a major portion of total AGB. More generally, palms are abundant members of many tropical forests, especially in the Neotropics, reaching upward of 60% relative basal area and sometimes forming dense monoculture stands with major contributions for carbon storage (Dalagnol et al., 2022; Hastie et al., 2022; Muscarella et al., 2020; Ter Steege et al., 2013). Although palms are monocots that lack true secondary growth, they exhibit sustained primary growth which can lead to coupled height–diameter relationships. Consequently, for at least some palm species, allometric models can be utilized to nondestructively estimate biomass from typical field-based measurements of stem diameter. Further work to develop species- and site-specific allometric models for palms that take into account a greater range of environmental heterogeneity, will be an important step to better understand tropical forest dynamics in response to disturbance, and to improve biomass estimates in tropical forests.

AUTHOR CONTRIBUTIONS
PC and RM designed the study, conducted the analysis, and drafted the manuscript. RL, JL, MU, and JKZ collected data. All authors reviewed the manuscript.

DATA AVAILABILITY STATEMENT
The data supporting the findings of this study are freely available through the Environmental Data Initiative (EDI) repository (Muscarella et al., 2023). The code used for the analysis and generation of results is freely available and reproducible within GitHub (Chatzopoulos & Muscarella, 2023). The repository can be accessed at [https://github.com/paschatz/PREMON_Palm-Allometry/tree/

v2.0.0]. Users are encouraged to refer to the README file for comprehensive instructions on replicating the analysis and results.

ORCID

Paschalis Chatzopoulos https://orcid.org/0000-0002-3456-7203

María Uriarte https://orcid.org/0000-0002-0484-0758

Robert Muscarella https://orcid.org/0000-0003-3039-1076

REFERENCES

Akaike, H. (1978). On the likelihood of a time series model. *Journal of the Royal Statistical Society Series D (The Statistician)*, 27, 217–235.

Antin, C., Pélissier, R., Vincent, G., & Couteron, P. (2013). Crown allometries are less responsive than stem allometry to tree size and habitat variations in an Indian monsoon forest. *Trees*, 27, 1485–1495.

Avalos, G., Cambronero, M., & Alvarez-Vergnani, C. (2022). Allometric models to estimate carbon content in Arecaceae based on seven species of Neotropical palms. *Frontiers in Forests and Global Change*, 5, 867912. https://doi.org/10.3389/ffgc.2022.867912

Avalos, G., Gei, M., Ríos, L. D., Otárola, M. F., Cambronero, M., Alvarez-Vergnani, C., Sylvester, O., & Rojas, G. (2019). Scaling of stem diameter and height allometry in 14 neotropical palm species of different forest strata. *Oecologia*, 190, 757–767.

Baccini, A., Goetz, S. J., Walker, W. S., Laporte, N. T., Sun, M., Sulla-Menashe, D., Hackler, J., Beck, P. S. A., Dubayah, R., Friedl, M. A., Samanta, S., & Houghton, R. A. (2012). Estimated carbon dioxide emissions from tropical deforestation improved by carbon-density maps. *Nature Climate Change*, 2, 182–185.

Burt, A., Calders, K., Cuni-Sanchez, A., Gómez-Dans, J., Lewis, P., Lewis, S. L., Malhi, Y., Phillips, O. L., & Disney, M. (2020). Assessment of bias in pan-tropical biomass predictions. *Frontiers in Forests and Global Change*, 3, 12. https://doi.org/10.3389/ffgc.2020.00012

Canham, C. D., Thompson, J., Zimmerman, J. K., & Uriarte, M. (2010). Variation in susceptibility to hurricane damage as a function of storm intensity in Puerto Rican tree species. *Biotropica*, 42, 87–94.

Chatzopoulos, P., & Muscarella, R. (2023). *Paschatz/PREMON_palm-Allometry: Height-diameter allometry for a dominant palm to improve understanding of carbon and forest dynamics in forests of Puerto Rico (v2.0.0)*. Zenodo. https://doi.org/10.5281/zenodo.10417497

Chave, J., Condit, R., Aguilar, S., Hernandez, A., Lao, S., & Perez, R. (2004). Error propagation and scaling for tropical forest biomass estimates. *Philosophical Transactions of the Royal Society of London. Series B, Biological Sciences*, 359, 409–420.

Chave, J., Réjou-Méchain, M., Búrquez, A., Chidumayo, E., Colgan, M. S., Delitti, W. B. C., Duque, A., Eid, T., Fearnside, P. M., Goodman, R. C., Henry, M., Martínez-Yrízar, A., Mugasha, W. A., Muller-Landau, H. C., Mencuccini, M., Nelson, B. W., Ngomanda, A., Nogueira, E. M., Ortiz-Malavassi, E., ... Vieilledent, G. (2014). Improved allometric models to estimate the aboveground biomass of tropical trees. *Global Change Biology*, 20, 3177–3190.

Clark, D. B., & Kellner, J. R. (2012). Tropical forest biomass estimation and the fallacy of misplaced concreteness. *Journal of Vegetation Science*, 23, 1191–1196.

Dalagnol, R., Wagner, F. H., Emilio, T., Streher, A. S., Galvão, L. S., Ometto, J. P. H. B., & Aragão, L. E. O. C. (2022). Canopy palm cover across the Brazilian Amazon forests mapped with airborne LiDAR data and deep learning. *Remote Sensing in Ecology and Conservation*, 8, 601–614. https://doi.org/10.1002/rse2.264

Duncanson, L., Armston, J., Disney, M., Avitabile, V., Barbier, N., Calders, K., Carter, S., Chave, J., Herold, M., Crowther, T. W., Falkowski, M., Kellner, J. R., Labrière, N., Lucas, R., MacBean, N., McRoberts, R. E., Meyer, V., Næsset, E., Nickeson, J. E., ... Williams, M. (2019). The importance of consistent global Forest aboveground biomass product validation. *Surveys in Geophysics*, 40, 979–999.

Duncanson, L. I., Dubayah, R. O., & Enquist, B. J. (2015). Assessing the general patterns of forest structure: Quantifying tree and forest allometric scaling relationships in the United States. *Global Ecology and Biogeography*, 24, 1465–1475.

Feldpausch, T. R., Banin, L., Phillips, O. L., Baker, T. R., Lewis, S. L., Quesada, C. A., Affum-Baffoe, K., Arets, E. J. M. M., Berry, N. J., Bird, M., Brondizio, E. S., de Camargo, P., Chave, J., Djagbletey, G., Domingues, T. F., Drescher, M., Fearnside, P. M., França, M. B., Fyllas, N. M., ... Lloyd, J. (2011). Height-diameter allometry of tropical forest trees. *Biogeosciences*, 8, 1081–1106.

Ferry, B., Morneau, F., Bontemps, J.-D., Blanc, L., & Freycon, V. (2010). Higher treefall rates on slopes and waterlogged soils result in lower stand biomass and productivity in a tropical rain forest. *Journal of Ecology*, 98, 106–116.

Frangi, J. L., & Lugo, A. E. (1985). Ecosystem dynamics of a subtropical floodplain Forest. *Ecological Monographs*, 55, 351–369.

Frangi, J. L., & Lugo, A. E. (1991). Hurricane damage to a flood plain Forest in the Luquillo Mountains of Puerto Rico. *Biotropica*, 23, 324–335.

Frangi, J. L., & Lugo, A. E. (1998). A floodplain palm forest in the Luquillo Mountains of Puerto Rico five years after hurricane Hugo. *Biotropica*, 30, 339–348.

Goodman, R. C., Phillips, O. L., del Castillo Torres, D., Freitas, L., Cortese, S. T., Monteagudo, A., & Baker, T. R. (2013). Amazon palm biomass and allometry. *Forest Ecology and Management*, 310, 994–1004.

Hastie, A., Honorio Coronado, E. N., Reyna, J., Mitchard, E. T. A., Åkesson, C. M., Baker, T. R., Cole, L. E. S., Oroche, C. J. C., Dargie, G., Dávila, N., de Grandi, E. C., del Águila, J., del Castillo Torres, D., de la Cruz Paiva, R., Draper, F. C., Flores, G., Grández, J., Hergoualc'h, K., Householder, J. E., ... Lawson, I. T. (2022). Risks to carbon storage from land-use change revealed by peat thickness maps of Peru. *Nature Geoscience*, 15, 369–374.

Herold, M., Carter, S., Avitabile, V., Espejo, A. B., Jonckheere, I., Lucas, R., McRoberts, R. E., Næsset, E., Nightingale, J., Petersen, R., Reiche, J., Romijn, E., Rosenqvist, A., Rozendaal, D. M. A., Seifert, F. M., Sanz, M. J., & De Sy, V. (2019). The role and need for space-based Forest biomass-related measurements in environmental management and policy. *Surveys in Geophysics*, 40, 757–778.

Johnson, J. B., & Omland, K. S. (2004). Model selection in ecology and evolution. *Trends in Ecology & Evolution*, 19, 101–108.

Johnston, M. H. (1992). Soil-vegetation relationships in a Tabonuco Forest Community in the Luquillo Mountains of Puerto Rico. *Journal of Tropical Ecology*, 8, 253–263.

KvaLseth, T. O. (1983). Note on the R2 measure of goodness of fit for nonlinear models. *Bulletin of the Psychonomic Society*, 21, 79–80.

Larjavaara, M., & Muller-Landau, H. C. (2013). Measuring tree height: A quantitative comparison of two common field methods in a moist tropical forest. *Methods in Ecology and Evolution*, 4, 793–801.

Ledo, A., Cornulier, T., Illian, J. B., Iida, Y., Kassim, A. R., & Burslem, D. F. R. P. (2016). Re-evaluation of individual diameter: Height allometric models to improve biomass estimation of tropical trees. *Ecological Applications*, 26, 2376–2382.

Lugo, A. E., & Frangi, J. L. (2016). Long-term response of Caribbean palm forests to hurricanes. *Caribbean Naturalist*, 1, 157–175.

Malhi, Y., Girardin, C., Metcalfe, D. B., Doughty, C. E., Aragão, L. E. O. C., Rifai, S. W., Oliveras, I., Shenkin, A., Aguirre-Gutiérrez, J., Dahlsjö, C. A. L., Riutta, T., Berenguer, E., Moore, S., Huasco, W. H., Salinas, N., da Costa, A. C. L., Bentley, L. P., Adu-Bredu, S., Marthews, T. R., ... Phillips, O. L. (2021). The global ecosystems monitoring network: Monitoring ecosystem productivity and carbon cycling across the tropics. *Biological Conservation*, 253, 108889.

Miller, G. L., & Lugo, A. E. (2009). *Guide to the ecological systems of Puerto Rico. General Technical Report* IITF-GTR-35. U.S. Department of

Agriculture, Forest Service, International Institute of Tropical Forestry.

Molto, Q., Rossi, V., & Blanc, L. (2013). Error propagation in biomass estimation in tropical forests. *Methods in Ecology and Evolution*, 4, 175–183.

Muscarella, R., Chatzopoulos, P., & Lammerant, R. (2023). Measurements of height, diameter at breast height and basal diameter for *Prestoea acuminata* at the Luquillo Forest dynamics plot (LFDP), Puerto Rico. ver 2. Environmental Data Initiative. https://doi.org/10.6073/pasta/7c635efb584b1d254d8b713361b13ad0

Muscarella, R., Emilio, T., Phillips, O. L., Lewis, S. L., Slik, F., Baker, W. J., Couvreur, T. L. P., Eiserhardt, W. L., Svenning, J. C., Affum-Baffoe, K., Aiba, S. I., de Almeida, E. C., de Almeida, S. S., de Oliveira, E. A., Álvarez-Dávila, E., Alves, L. F., Alvez-Valles, C. M., Carvalho, F. A., Guarin, F. A., … Balslev, H. (2020). The global abundance of tree palms. *Global Ecology and Biogeography*, 29, 1495–1514.

Niklas, K. J. (1992). *Plant biomechanics: An engineering approach to plant form and function*. University of Chicago Press.

Niklas, K. J. (2004). Plant allometry: Is there a grand unifying theory? *Biological Reviews of the Cambridge Philosophical Society*, 79, 871–889.

Ogle, D. H., Doll, J. C., Wheeler, A. P., & Dinno, A. (2023). FSA: Simple Fisheries Stock Assessment Methods. Available at: https://CRAN.R-project.org/package=FSA

R Development Core Team. (2020). *R: A language and environment for statistical computing*. R Foundation for Statistical Computing Available from: http://www.R-project.org

Réjou-Méchain, M., Tanguy, A., Piponiot, C., Chave, J., & Hérault, B. (2017). Biomass: An R package for estimating above-ground biomass and its uncertainty in tropical forests. *Methods in Ecology and Evolution*, 8, 1163–1167.

Smith, C. (2022). EDIutils: An API Client for the Environmental Data Initiative Repository. Available from: https://zenodo.org/record/6612472

Sprugel, D. G. (1983). Correcting for bias in log-transformed allometric equations. *Ecology*, 64, 209–210.

Sullivan, M. J. P., Lewis, S. L., Affum-Baffoe, K., Castilho, C., Costa, F., Sanchez, A. C., Ewango, C. E. N., Hubau, W., Marimon, B., Monteagudo-Mendoza, A., Qie, L., Sonké, B., Martinez, R. V., Baker, T. R., Brienen, R. J. W., Feldpausch, T. R., Galbraith, D., Gloor, M., Malhi, Y., … Phillips, O. L. (2020). Long-term thermal sensitivity of Earth's tropical forests. *Science*, 368, 869–874.

Ter Steege, H., Pitman, N. C. A., Sabatier, D., Baraloto, C., Salomão, R. P., Guevara, J. E., Phillips, O. L., Castilho, C. V., Magnusson, W. E., Molino, J. F., Monteagudo, A., Núñez Vargas, P., Montero, J. C., Feldpausch, T. R., Coronado, E. N. H., Killeen, T. J., Mostacedo, B., Vasquez, R., Assis, R. L., … Silman, M. R. (2013). Hyperdominance in the Amazonian tree flora. *Science*, 342, 1243092.

Thompson, J., Brokaw, N., Zimmerman, J. K., Waide, R. B., Everham, E. M., Lodge, D. J., Taylor, C. M., García-Montiel, D., & Fluet, M. (2002). Land use history, environment, and tree composition in a tropical forest. *Ecological Applications*, 12, 1344–1363.

Tomlinson, P. B. (1990). *The structural biology of palms*. CLAREDON PRESS.

Uriarte, M., Canham, C. D., Thompson, J., & Zimmerman, J. K. (2004). A neighborhood analysis of tree growth and survival in a hurricane-driven tropical forest. *Ecological Monographs*, 74, 591–614.

Uriarte, M., Tang, C., Morton, D. C., Zimmerman, J. K., & Zheng, T. (2023). 20th-century hurricanes leave long-lasting legacies on tropical forest height and the abundance of a dominant wind-resistant palm. *Ecology and Evolution*, 13, e10776. https://doi.org/10.1002/ece3.10776

Uriarte, M., Thompson, J., & Zimmerman, J. K. (2019). Hurricane María tripled stem breaks and doubled tree mortality relative to other major storms. *Nature Communications*, 10, 1362.

Weaver, P. L. (2010). Forest structure and composition in the lower montane rain forest of the Luquillo mountains, Puerto Rico. *Interciencia*, 35, 640–646.

Weiner, J. (2004). Allocation, plasticity and allometry in plants. *Perspectives in Plant Ecology, Evolution and Systematics*, 6, 207–215.

Xu, Y., & Goodacre, R. (2018). On splitting training and validation set: A comparative study of cross-validation, bootstrap and systematic sampling for estimating the generalization performance of supervised learning. *Journal of Analysis and Testing*, 2, 249–262.

Zhang, J., Bras, R. L., Longo, M., & Heartsill Scalley, T. (2022a). The impact of hurricane disturbances on a tropical forest: Implementing a palm plant functional type and hurricane disturbance module in ED2-HuDi V1.0. *Geoscientific Model Development*, 15, 5107–5126.

Zhang, J., Bras, R. L., Longo, M., & Heartsill Scalley, T. (2022b). Future hurricanes will increase palm abundance and decrease aboveground biomass in a tropical forest. *Geophysical Research Letters*, 49, e2022GL100090. https://doi.org/10.1029/2022GL100090

Zimmerman, J. (2018). Physical environment of the Luquillo Forest dynamics plot (LFDP), Puerto Rico ver 381051. Environmental data initiative. https://doi.org/10.6073/pasta/c0b8fef481d7bf2825341b3839b085a0

Zimmerman, J. K., Wood, T. E., González, G., Ramirez, A., Silver, W. L., Uriarte, M., Willig, M. R., Waide, R. B., & Lugo, A. E. (2021). Disturbance and resilience in the Luquillo experimental Forest. *Biological Conservation*, 253, 108891.

Zuleta, D., Krishna Moorthy, S. M., Arellano, G., Verbeeck, H., & Davies, S. J. (2022). Vertical distribution of trunk and crown volume in tropical trees. *Forest Ecology and Management*, 508, 120056.

SUPPORTING INFORMATION

Additional supporting information can be found online in the Supporting Information section at the end of this article.

How to cite this article: Chatzopoulos, P., Lammerant, R., Thompson, J., Uriarte, M., Zimmerman, J. K., & Muscarella, R. (2024). Height–diameter allometry for a dominant palm to improve understanding of carbon and forest dynamics in forests of Puerto Rico. *Biotropica*, 00, 1–12. https://doi.org/10.1111/btp.13297